



Optimization of reasonable production pressure difference of multiple-fractured horizontal well in fractured tight reservoir

Yu Wang¹ · Yuetian Liu¹ · Lu Sun¹

Received: 13 November 2018 / Accepted: 8 March 2019 / Published online: 26 April 2019
© Saudi Society for Geosciences 2019

Abstract

There is pressure-sensitive effect in the development of tight reservoirs, so we need to optimize the reasonable production pressure difference. This paper determined the main controlling factors of reasonable production pressure difference and provided guidance for optimal design of production pressure difference. Based on Green's function and source/sink method, a semi-analytical productivity model of multiple-fractured horizontal well (MFHW) considering the pressure-sensitive effect of artificial fractures and natural fractures is established, which can be used to predict the unstable productivity of MFHWs and analyze the effect of parameters on productivity and reasonable production pressure difference. Modeling results are compared with those from numerical model built by software CMG, obtaining a good match. Afterwards, sensitivity analysis was done in the work, three key parameters are analyzed: (1) pressure-sensitive coefficient of artificial fracture, (2) compressibility of natural fracture network, and (3) direction of principal permeability. The results show that the reasonable production pressure difference is mainly related to the pressure-sensitive coefficient of artificial fractures. By contrast, the difference of compression coefficient between natural fractures and direction of principal permeability has a small impact on reasonable production pressure difference. Finally, the proposed model is used to calculate the reasonable production pressure difference of JHW015 in Xinjiang oilfield and the reasonable production pressure difference of JHW015 is 8.4 MPa. The model considering the pressure-sensitive effect of artificial and natural fractures can predict oil production more accurately, which can provide the important evidences for reasonable production difference pressure and fracturing optimization design in tight reservoir.

Keywords Tight reservoirs · MFHW · Production pressure difference

Introduction

In recent years, unconventional reservoirs have gained great attention all over the world. Multiple hydraulic-fracturing techniques which can induce fractures with high conductivity have been applied successfully in a number of oil and gas fields. Tight reservoirs belong to unconventional resources. At present, because of the complex interplay of flow among matrix, natural fractures, hydraulic fractures, and horizontal

wellbore, productivity prediction in tight reservoirs is the key and a difficult task for the reservoir engineers.

Many scholars have studied the productivity prediction of MFHWs. Giger et al. (1984) presented the first mathematical model for analyzing productivity of MFHWs. However, the model does not rigorously couple the flow in the reservoir and in the fracture. And then Karcher et al. (1986) and Soliman et al. (1990) improved Giger's model. Gringarten et al. (1974) predicted the unsteady-state pressure behavior of a well with a single infinite conductivity vertical fracture in infinite and bounded reservoirs. Afterwards, Cinco-Ley and Samaniego-V (1981) presented a new technique to analyze pressure transient data for finite conductivity vertical fractures by using bilinear flow analysis. Pressure loss in long horizontal wells cannot be ignored. A productivity model was first presented by Yildiz and Ozkan (1998) to predict the horizontal well performance with multi-fracturing, which considered a finite conductivity horizontal well. Wan and Aziz (2002) presented a semi-analytical well model for horizontal wells with multiple hydraulic fractures, which can consider more complex

This article is part of the Topical Collection on *Geo-Resources-Earth-Environmental Sciences*

✉ Yu Wang
wangyu199311@126.com

✉ Yuetian Liu
lyt51@163.com

¹ State Key Laboratory of Petroleum Resources and Prospecting, China University of Petroleum (Beijing), Beijing, China

factors than analytical models. As for fluid flow, many models were presented by Li et al. (1996) and Wei and Economides (2005) that couple the reservoir linear flow, fracture linear flow, and fracture radial flow. Guo and Schechter (1997) presented a mathematical model coupling the reservoir linear flow and fracture linear flow. Mayerhofer et al. (2010) proposed that multi-fracturing can create complex fracture network in SVR. He indicated that SRV is necessary for describing the stimulation performance. Yao and Zeng (2013) presented the reservoir/fractures/wellbore coupling model based on plan/slab source solution in a box-shaped reservoir and pressure drop in hydraulic fractures and horizontal wellbore are also considered. Ozkan and Brown (2013) established a trilinear-flow model based on the premise that the drainage volume is limited to the reservoir volume between hydraulic fractures, to further simulate the performances of MFHWs. Zhang and Yang (2018) presented semi-analytical model describing the non-Darcy flow in the fracture, which can improve the accuracy of productivity. Guo et al. (2015) analyzed the effect of fracture width on the long-term productivity of fractured wells, in his study, artificial fracture is wedge. He and Cheng (2017) developed a new model for MFHWs in a tight gas reservoir, and to further investigate the effects of fracture properties on pressure response, which improved well performance by stimulation measures. Zeng and Wang (2016) presented an analytical model for MFHWs with consideration of TPG, partially penetrating fractures, and reservoir heterogeneity, and further analyzed the effects of parameters. Tian and Feng (2019) predicted reservoir performance by coupling the dynamic capillary pressure with gas production models. He and Cheng (2018) presented an improved rate-transient analysis (RTA) model of MFHWs, and investigated the effects of non-uniform properties of hydraulic fractures on transient rate behaviors. To sum up, productivity models take into account seepage characteristics, fluid phase, inter-fracture interference, fracture morphology and fracture conductivity, wellbore pressure drop, non-Darcy flow, dynamic and capillary pressure comprehensively.

There are a large number of fracture networks in SRV region, which is a pressure-sensitive region. Meanwhile, field practice shows that the effect of pressure-sensitive effect on productivity is great. Therefore, it is essential to establish a productivity model of MFHW considering the pressure-sensitive effect of artificial fractures and natural fractures and to analyze the influence of natural fracture networks on productivity in tight reservoirs and eventually to optimize the reasonable production pressure difference.

This study is focused on the pressure-sensitive effect in tight reservoir, including artificial fracture and natural fracture networks. And a productivity model of MFHW in tight reservoirs considering the pressure-sensitive effect of artificial fractures and natural fractures is established. What's more, this work provides a good understanding of the influence of key

parameters on the productivity and reasonable production pressure difference, which is helpful to provide an important guidance for the optimal design of reasonable production pressure difference in tight reservoirs.

Methodology

Physical model

As shown in Fig. 1, a model of MFHW is established. To make the physical model better understood, the whole model is divided into three parts: (1) reservoir (including natural fracture networks), (2) artificial fracture, and (3) horizontal wellbore.

And for mathematical simplicity, the following assumptions are made:

- The MFHW is located in a box-shaped reservoir and all the boundaries are closed boundaries.
- The horizontal wellbore is parallel to the reservoir boundary.
- The artificial fractures are vertical, symmetrical, and perpendicular to the horizontal well. The artificial fractures are successively marked $f_1, f_2, f_3, \dots, f_N$. The wedge model is used to describe the width of artificial fractures.
- The model is derived for single-phase flow.
- The flow process is reservoir-fracture-wellbore. The fluid flow from the reservoir directly to the horizontal wellbore is ignored.
- There are many groups of high-angle fractures whose direction and spacing are similar in the reservoir.
- The reservoir is anisotropic because of the existence of natural fracture networks.

Based on the above assumptions, the model has the following limitations:

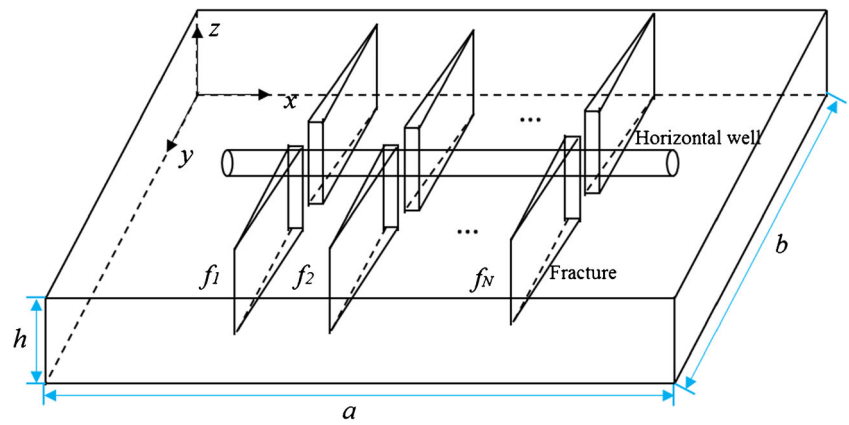
- The model cannot describe the three-dimensional morphology of the artificial fractures, ignoring inclination and direction.
- Natural fractures have only statistical direction and spacing, and actual flow process cannot be described.
- The model, ignoring the fluid flow from the reservoir directly to the horizontal wellbore, is only used for MFHWs with casing completion.

Based on these assumptions and limitations, the three parts will be discussed in detail.

Artificial fracture

As shown in Fig. 2, taking the k th artificial fracture as an example, each fracture is divided into multiple sink units.

Fig. 1 Schematic of MFHW in box-shaped reservoir



According to the research of finite conductivity fractured vertical wells, the pressure drop between the j th sink unit and the grid of wellbore is

$$P_{k1,j} - P_{k1,0} = \int_{y_j}^{y_0} \frac{q\mu}{K_f w_f h} dy = \sum_{i=1}^j \frac{q_{k1,i} \mu \Delta y_{f_{k1,i}}}{K_f w_{f_{k1,i}} h} \quad (1)$$

The flow in the grid of wellbore is considered as radial flow, and the Peaceman's (1990) wellbore flow model is adopted.

$$P_{k1,0} - P_{wf} = \frac{q\mu[\ln(r_o/r_w) - 0.5]}{2\pi Kh} \quad (2)$$

where r_o is equivalent grid radius,

$$r_o = 0.14(\Delta y^2 + h^2). \quad (3)$$

The width of i th unit is

$$w_{fki} = w_{f_{kmin}} + (2i-1)(w_{f_{kmax}} - w_{f_{kmin}})/(2ns) \quad (4)$$

where $w_{f_{kmax}}$ is the width of fracture heel and $w_{f_{kmin}}$ is the width of fracture toe.

Besides, the pressure-sensitive effect in artificial fractures cannot be ignored. Based on a large number of experimental studies, the permeability of artificial fractures and pressure have exponential function relations:

$$k_{AF} = k_{AF0} e^{\alpha_{AF}(P - P_{mi})} \quad (5)$$

where k_{AF} is the permeability of the artificial fracture, α_{AF} is pressure-sensitive coefficient of artificial fracture.

Reservoir (natural fracture networks)

Natural fractures are different from artificial fracture, as shown in Fig.3; artificial fracture is a single fracture and natural fractures are fracture networks consisting of multiple groups of fractures. Natural fractures are scattered disorderly in reservoirs. It is generally believed that the formation of natural fractures is related to crustal stress. Therefore, the direction of natural fractures has certain regularity. In order to consider the influence of natural fractures in the model, based

Fig. 2 Schematic diagram of the flow model in a fracture

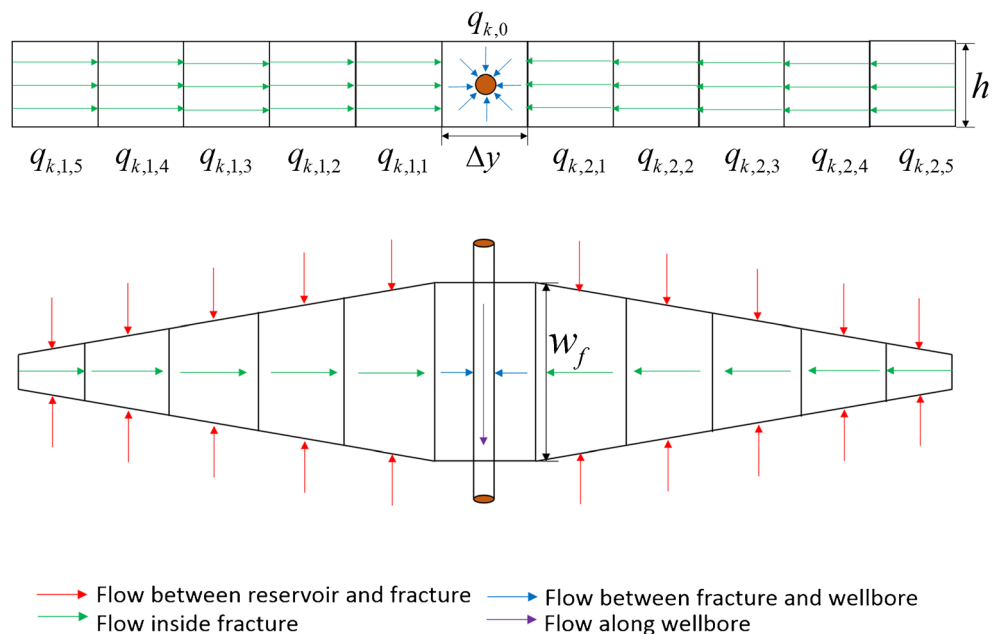
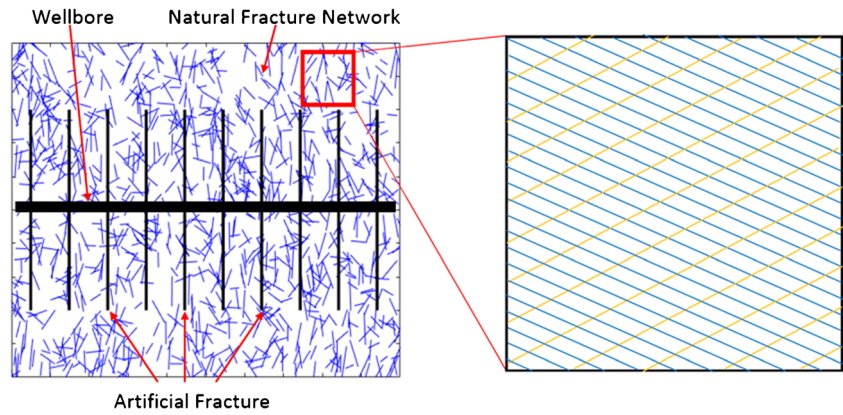


Fig. 3 Complex fracture network distribution and simplified schematic diagram in SRV region



on the geo-statistical results, natural fractures can be abstractly divided into several groups with respective parameters such as compressibility, aperture, direction, and density. And the permeability tensor based on multi-group fracture network is established and applied to the productivity model.

Ma et al. (2013) studied that when there is N group of fractures in reservoir, the permeability tensor considering the influence N group of fractures is obtained by Eq. 6.

$$K = \sum_{i=1}^N \begin{bmatrix} k_m + \frac{1 + \cos 2\beta_i}{2} k_{fi} & \frac{k_{fi} \sin 2\beta_i}{2} \\ \frac{k_{fi} \sin 2\beta_i}{2} & k_m + \frac{1 - \cos 2\beta_i}{2} k_{fi} \end{bmatrix} \quad (6)$$

where β_i is the angle between the i th group of natural fracture network and the x -axis, the clockwise is positive, and the clockwise is negative. k_m is matrix permeability, and k_{fi} is the permeability of the i th group of natural fracture network.

In order to accurately characterize the pressure-sensitive effect of natural fracture network and matrix, Du and Wong have studied and established the pressure-sensitive formula.

$$k_{fi} = k_{fi0} \left(1 + \frac{C_f \Delta P}{\phi} \right)^3 \quad k_m = k_{m0} \left(1 - \frac{C_f \Delta P}{\phi} \right)^2 \quad (7)$$

$$K = \sum_{i=1}^N \begin{bmatrix} k_{m0} \left(1 + \frac{C_f \Delta P}{\phi} \right)^2 + \frac{1 + \cos 2\beta_i}{2} k_{fi0} \left(1 + \frac{C_f \Delta P}{\phi} \right)^3 & \frac{k_{fi0} \left(1 + \frac{C_f \Delta P}{\phi} \right)^3 \sin 2\beta_i}{2} \\ \frac{k_{fi0} \left(1 + \frac{C_f \Delta P}{\phi} \right)^3 \sin 2\beta_i}{2} & k_{m0} \left(1 + \frac{C_f \Delta P}{\phi} \right)^2 + \frac{1 - \cos 2\beta_i}{2} k_{fi0} \left(1 + \frac{C_f \Delta P}{\phi} \right)^3 \end{bmatrix} \quad (8)$$

where C_{fi} is the compression coefficient of i th group of natural fractures, ΔP is pressure difference $\Delta P = p - p_{ini}$.

Then, the full tensor $K' = \begin{bmatrix} k'_{xx} & k'_{xy} \\ k'_{yx} & k'_{yy} \end{bmatrix}$ can be converted

to diagonal tensor $K = \begin{bmatrix} k_{xx} & \\ & k_{yy} \end{bmatrix}$.

$$K = \begin{bmatrix} \frac{k'_{xx} + k'_{yy}}{2} + \frac{k'_{xx} - k'_{yy}}{2} \cos 2\gamma + k'_{xy} \sin 2\gamma & \\ & \frac{k'_{xx} + k'_{yy}}{2} - \frac{k'_{xx} - k'_{yy}}{2} \cos 2\gamma - k'_{xy} \sin 2\gamma \end{bmatrix} \quad (9)$$

where γ is the angle between the two coordinate systems

$$\gamma = \frac{1}{2} \arctan \left(\frac{2k'_{xy}}{(k'_{xx} - k'_{yy})} \right) \quad (10)$$

The research shows that the value of principal permeability will change with the change of pressure in elastic isotropic media; however, in elastic anisotropic media, which means different compression coefficients C_{fi} of natural fracture networks, not only will the value of principal permeability change, but also the direction of principal permeability will change, which will affect the productivity in tight reservoir. The change of principal permeability with pressure is shown in Fig. 4. Based on the above research, the productivity model of MFHWs in fractured tight reservoirs should consider the direction change of the principal permeability due to natural fracture networks.

In view of the inconsistency between the direction of principal permeability and the reference coordinate system, as shown in Fig. 5, the angle is α , which cannot be solved by the method that the direction of principal permeability is consistent with the direction of the reference coordinate system. In the study, Schwarz-Christoffel transform was used, the size of the reservoir boundary and the location of the sink unit will change, and the direction of the principal permeability is consistent with the direction of the reference coordinate system.

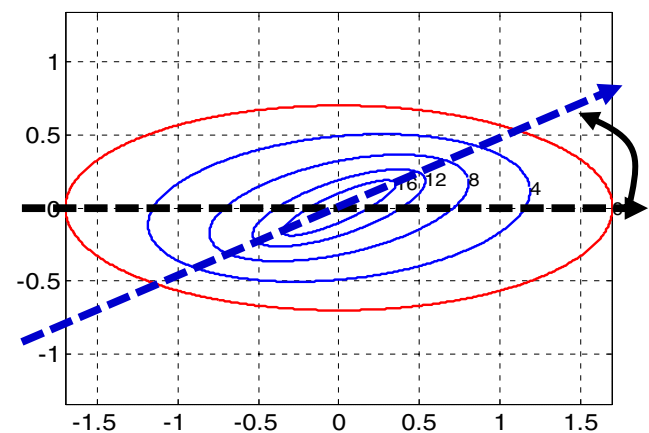
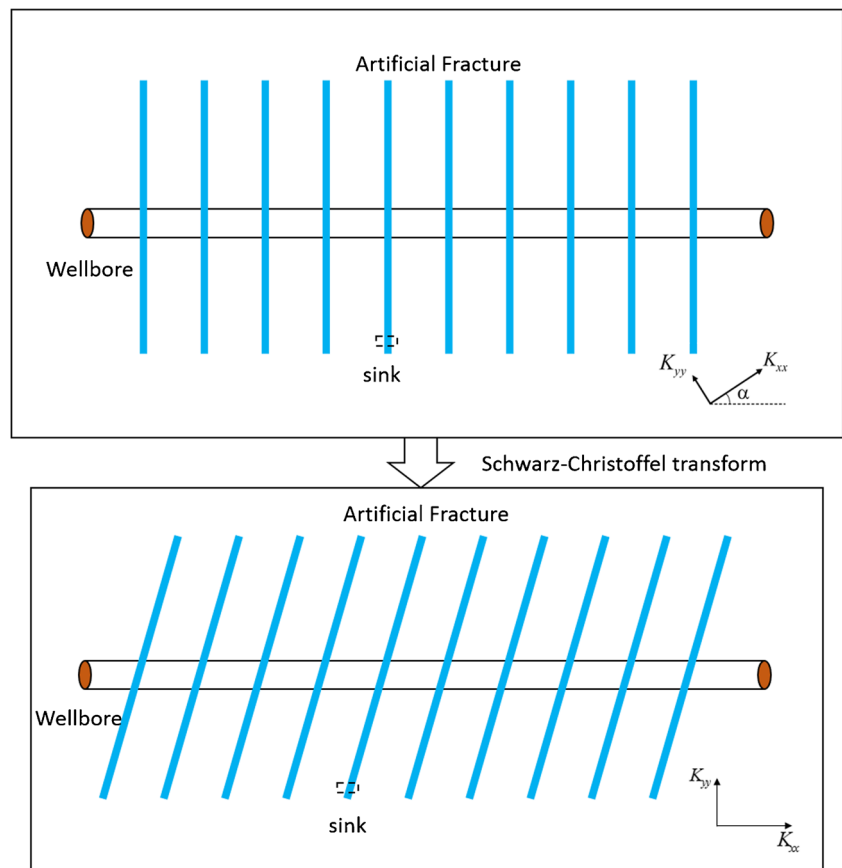


Fig. 4 Deformation characteristic of permeability tensor with the reduction of pressure

Fig. 5 Schematic of Schwarz-Christoffel transform



Based on the results of Penmatcha (1997), from $t_0 = 0$ to t , fluid flow into artificial fractures on the all the sink units at

different flow rates $q_{k1, i}$, causing the pressure drop at the point $(x_{k1, j}, y_{k1, j}, z_{k1, j})$ is

$$\Delta p(x_{k1,j}, y_{k1,j}, z_{k1,j}, t) = p_{ini} - p_{k1,j} = \sum_{s=1}^N \left(\sum_{i=1}^{ns} (\Delta p_{s1,i} + \Delta p_{s2,i}) \right) \tag{11}$$

$$= \frac{1}{abh\phi C_t} \sum_{s=1}^N \left(\sum_{i=1}^{ns} \left(q_{s1,i} \int_0^t (S_1 \cdot S_2 \cdot S_3)_{s1,i} d\tau + q_{s2,i} \int_0^t (S_1 \cdot S_2 \cdot S_3)_{s2,i} d\tau \right)_{(x_{k1,j}, y_{k1,j}, z_{k1,j})} \right)$$

where S_1 , S_2 , and S_3 represent Green's function of the point $(x_{k1, i}, y_{k1, i}, z_{k1, i})$, the detailed source functions in Appendix.

$$\Delta p_{fi} = \frac{f_i q_i^2 \rho l_i}{4\pi r_w^2} \tag{12}$$

Wellbore

for laminar flow,

Based on Chen and Liao's (2017) study, the pressure drop within wellbore is mainly caused by four components: (1) the acceleration pressure drop, (2) the frictional pressure drop, (3) the inflow directional pressure drop, and (4) the gravitational pressure drop.

$$N_{Re} < 2100 : f_i = \frac{64}{N_{Re}} \tag{13}$$

As shown in Fig. 6, in this work, component 3 and component 4 are neglected. Then, we only take the acceleration and frictional pressure drops into account.

for turbulent flow,

$$N_{Re} > 2000 : \frac{1}{\sqrt{f_i}} = -4.0 \log \left[\frac{\varepsilon}{3.7D} + \frac{1.255}{\sqrt{f_i} N_{Re}} \right] \tag{14}$$

The frictional pressure loss results from the frictional resistance within the wellbore, which can be calculated with friction factor as below:

where

$$N_{Re} = 0.1231 \times \frac{q_i \rho}{\mu d} \tag{15}$$

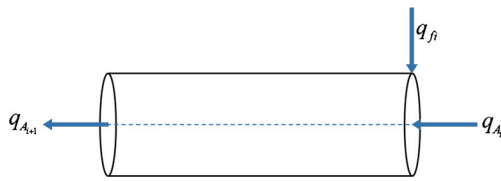


Fig. 6 Schematic diagram of *i*th wellbore unit

The acceleration pressure drop is caused by kinetic energy change. Along the horizontal wellbore, the fluid velocity becomes bigger and bigger. On the basis of hydrodynamics theory (Baba and Tiab 2001), the acceleration pressure drop is expressed as

$$\Delta p_{ai} = F_{ai}/A = \rho(v_{i2}^2 - v_{i1}^2) = \rho \left(\frac{q_{fi}^2 + 2q_{fi}q_{Ai}}{\pi^2 r_w^4} \right). \tag{16}$$

Model coupling and solution

Taking fracture f_k as an example, the pressure drop caused by the fluid flow in the reservoir is equal to which caused by the fluid flow in the fracture. The coupled flow equation of reservoir-fracture-wellbore is established:

$$p_{ini} - p_{wf} = \sum_{i=1}^j \frac{q_{k1,i} \mu \Delta y_{f_{k1,i}}}{K_f w_{f_{k1,i}} h} + \frac{q_k \mu [\ln(r_o/r_w) - 0.5]}{2\pi K_f h} + C \sum_{s=1}^N \left(\sum_{i=1}^{ns} \left(q_{s1,i} \int_0^{n\Delta t} (S_1 \cdot S_2 \cdot S_3)_{s1,i} d\tau + q_{s2,i} \int_0^{n\Delta t} (S_1 \cdot S_2 \cdot S_3)_{s2,i} d\tau \right)_{(x_{k1,j}, y_{k1,j}, z_{k1,j})} \right) \tag{17}$$

where $q_k = \sum_{i=1}^{ns} q_{k1,i} + \sum_{i=1}^{ns} q_{k2,i}$

In total, there are $2ns \times N$ linear equations, which can be expressed as $A \cdot q_{n\Delta t} = B$. The coefficient matrix A and vector B are shown in Appendix. By solving equations, the vector $q_{n\Delta t}$ at the step of $n\Delta t$ can be obtained whose expression is

$$q_{n\Delta t} = [q_{(1)}, q_{(2)}, \dots, q_{(k)}, \dots, q_{(N)}]_{n\Delta t}^T$$

where

$$q_{(k)} = [q_{(k)1,1}, q_{(k)1,2}, \dots, q_{(k)1,ns}, q_{(k)2,1}, q_{(k)2,2}, \dots, q_{(k)2,ns}]_{n\Delta t}^T \tag{18}$$

The procedure of coupling all solutions to generate a linear equation system is shown in Fig. 7. Since the pressure

calculation in the horizontal well is based on the flow rate inside the wellbore which we are seeking for, iterative process is needed to approach the accurate results.

Model Verification

In this work, the numerical simulator CMG is used to verify the proposed model with an MFHW. The basic parameters are shown in Table 1. Then, a numerical model with an MFHW is built by CMG, as shown in Fig. 8. In the numerical model, the reservoir with a domain of $2000\text{m} \times 500\text{m} \times 10\text{m}$ is modeled by $80 \times 25 \times 10$ grids. To accurately simulate the flow within or into the fracture, logarithmic refined grids are used in the vicinity of the fracture. The permeability tensor in the

Fig. 7 Flow chart for modeling and solving process

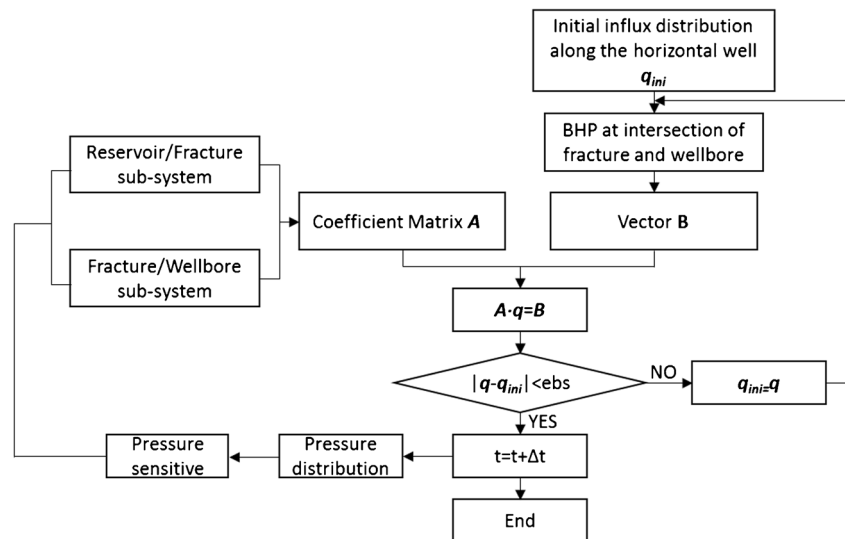


Table 1 Basic parameters for model

Parameters	Value
Reservoir size	2000 m × 500 m × 10 m
Permeability of artificial fractures	90 μm ²
Aperture of artificial fractures (heel and toe)	6 mm, 2.5 mm
Half-length of artificial fractures	100 m
Pressure-sensitive coefficient of artificial fractures	0.15 MPa ⁻¹
Length of horizontal wellbore	1300 m
Number of stages	18
Direction of two sets of natural fracture (North: 0° clockwise)	30°, 90°
Compression coefficient of two sets of natural fracture	0.002 MPa ⁻¹ , 0.003 MPa ⁻¹
Permeability of two sets of natural fracture	1 × 10 ⁻³ μm ² , 1 × 10 ⁻³ μm ²
Matrix permeability	0.01 × 10 ⁻³ μm ²
Matrix porosity	0.16
Initial reservoir pressure	47.36 MPa
Bottom hole pressure	38.70 MPa
Oil viscosity	8.5 mPa s
Production time	600 days

Fig. 8 Numerical model of an MFHW built by CMG

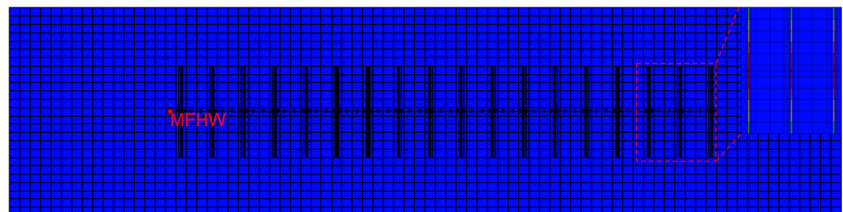


Fig. 9 Comparison between our modeling results and those in numerical model

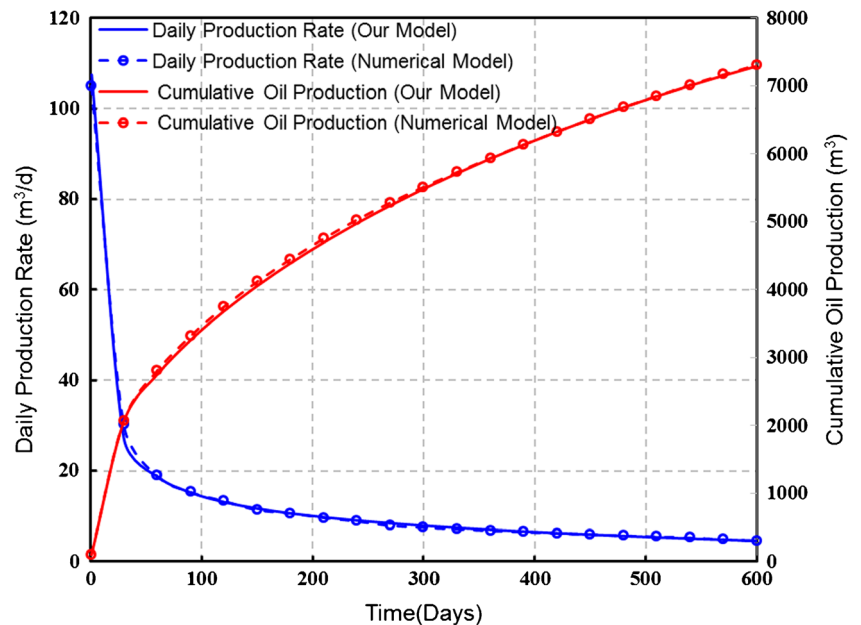
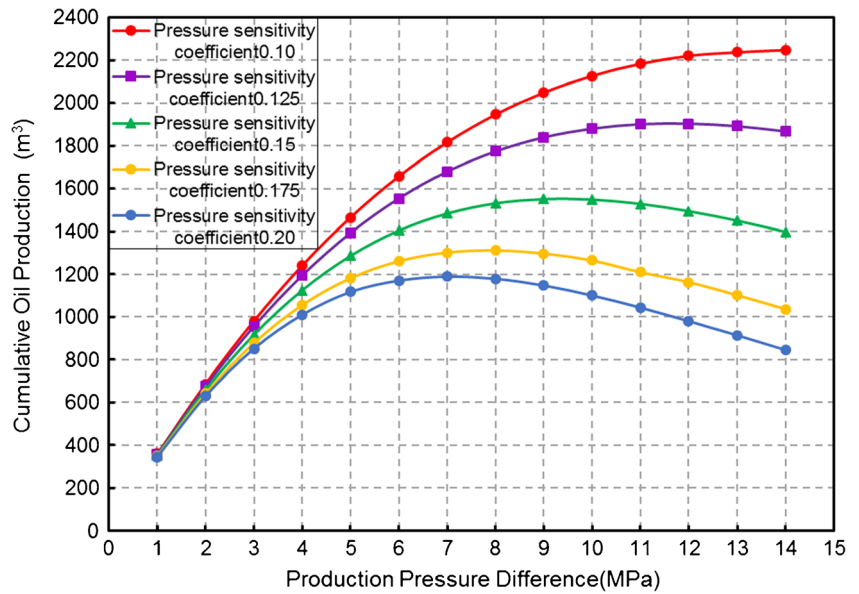


Fig. 10 Cumulative oil production under different production pressure difference (stress-sensitivity coefficient of artificial fracture)



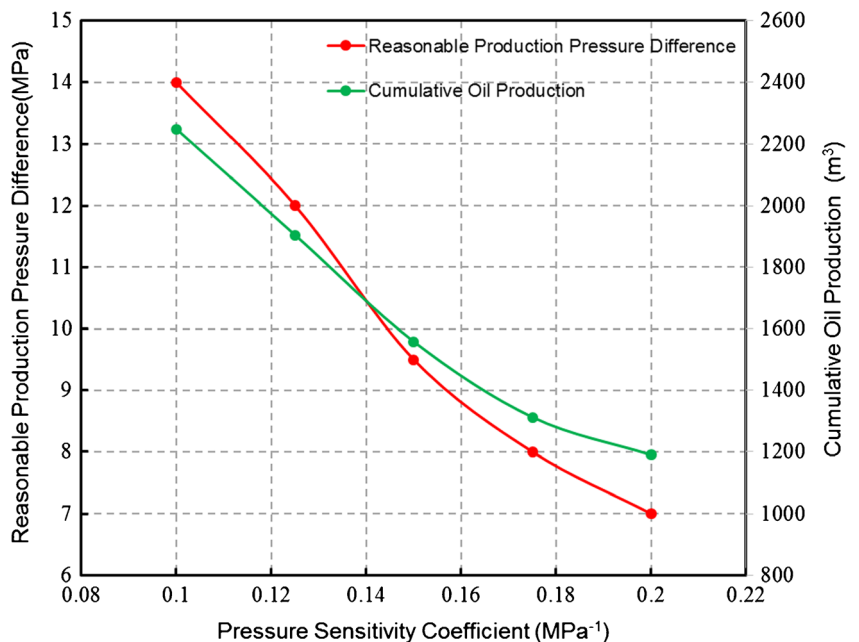
numerical model is calculated by formula 6, and the reservoir model is single-phase flow.

After a comparison of daily production rate and cumulative oil production, as shown in Fig. 9, it is found that our modeling results match well with numerical results, which indicates that our model can be used to predict the production in an MFHW and analyze parameters sensitivity.

Sensitivity analysis

The emphasis of this study is to discuss the effect of the artificial fracture and the fracture network in SRV area on

Fig. 11 Reasonable production pressure difference and cumulative oil production under different pressure-sensitive coefficient

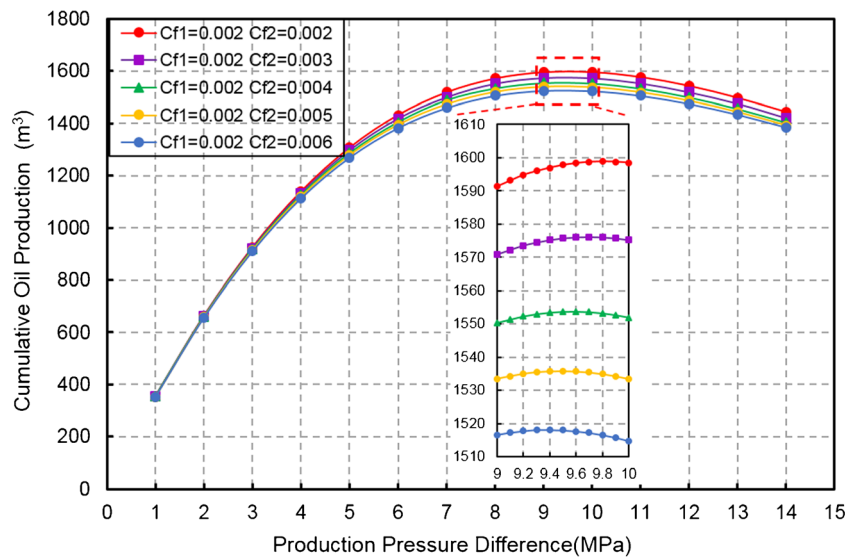


cumulative oil production and reasonable production pressure difference; therefore, the following three key parameters are analyzed: pressure-sensitive coefficient of artificial fracture, compressibility of natural fracture network, and direction of principal permeability.

Pressure-sensitive coefficient of artificial fracture

In Fig. 10, the relationship between cumulative oil production and production pressure difference under different pressure-sensitive coefficient of artificial fracture is presented. By comparing different curves, we can find that the larger the pressure-sensitive coefficient, the lower the cumulative oil

Fig. 12 Cumulative oil production curves under different pressure difference (compressibility of natural fracture network)



production. When pressure-sensitive coefficient is equal to 0.10, the cumulative oil production increases as production pressure difference increases; however, the rate of increase has slowed down. Relatively, when pressure-sensitive coefficient is larger than 0.10, with the increase of pressure difference, the cumulative oil production increases first and then decreases, that is, there is a reasonable production pressure difference to maximize the cumulative oil production.

Based on the data in Fig. 10, the optimal production pressure difference under different pressure-sensitive coefficient of artificial fracture is plotted. As shown in Fig. 11, the larger the pressure-sensitive coefficient of artificial fracture is, the smaller the reasonable production pressure difference is, and the smaller the cumulative oil production is.

The pressure-sensitive coefficient of artificial fracture changes from 0.100 to 0.200 MPa⁻¹, and the optimal production pressure decreases from 14 to 7 MPa. The cumulative oil production decreases from 2248.20 to 1189.94 m³, which reduces by 47.07%. As a result, we can conclude that pressure-sensitive effect of artificial fracture plays a key role in determining reasonable production pressure difference and cumulative oil production.

Compressibility of natural fracture network

According to the research of Du and Wong (2002), it is mentioned that when there are multiple fractures with the

Fig. 13 Reasonable production pressure difference and cumulative oil production under different compressibility of natural fracture network

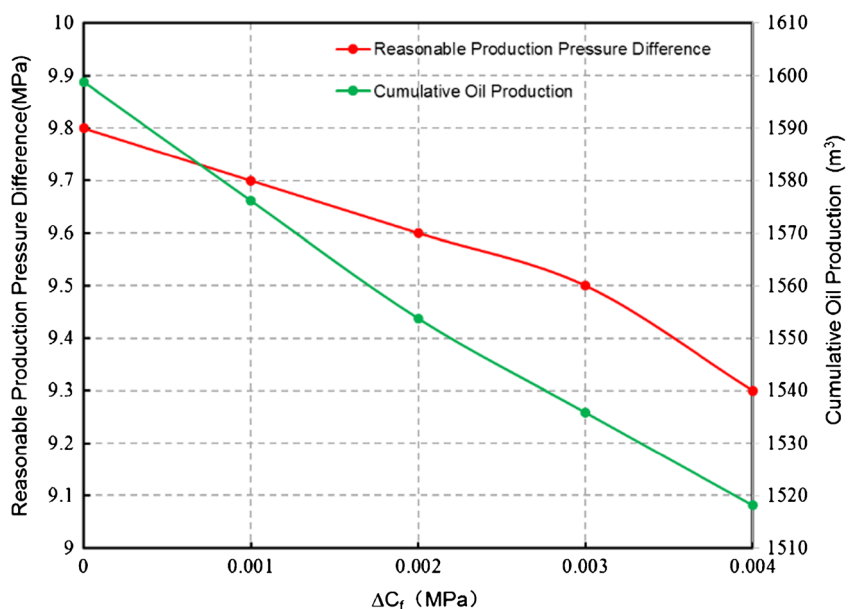
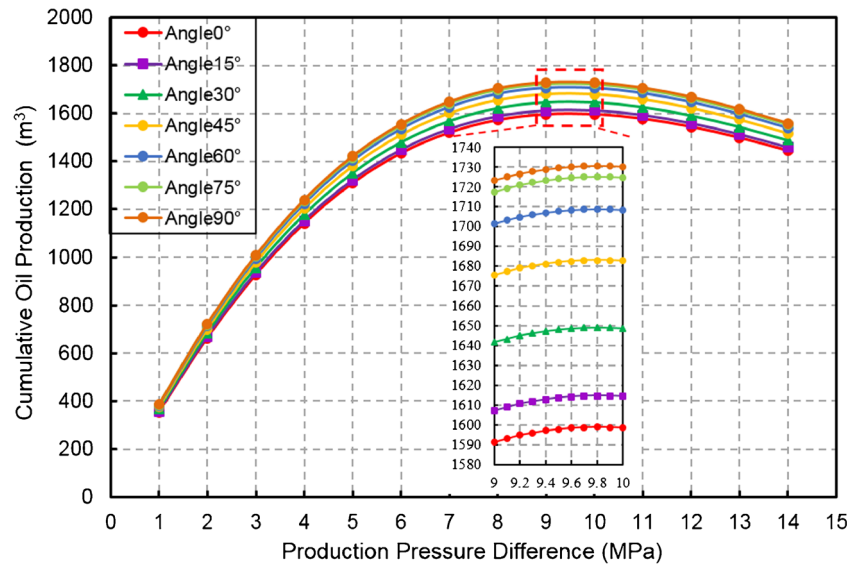


Fig. 14 Cumulative oil production curves under different pressure difference (direction of principal permeability)



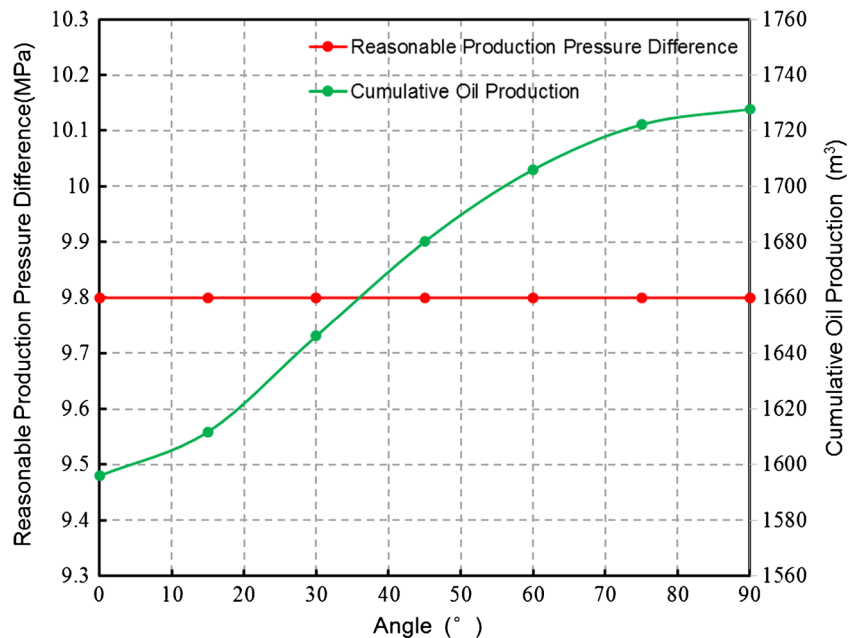
difference of elastic parameters in reservoir, with the change of pressure, not only will the value of principal permeability change, but also the direction of principal permeability will change. Therefore, we set the pressure-sensitive coefficient of artificial fracture to be 0.15 firstly and then assume that there are two groups of natural fracture networks with different compression coefficients— C_{f1} and C_{f2} . The direction of two groups of natural fracture networks is -30° and 30° (North is 0° , clockwise is positive) respectively, which means the angle between the initial principal permeability and the artificial fracture is 0° .

Afterwards, we set the C_{f1} to be 0.002 MPa^{-1} , and set the C_{f2} to be 0.002 MPa^{-1} , 0.003 MPa^{-1} , 0.004 MPa^{-1} , 0.005 MPa^{-1} , and 0.006 MPa^{-1} respectively. Then, the

relationship between cumulative oil production and production pressure difference is obtained.

As shown in Fig. 12, the trend of the five curves is almost the same, which means that the difference of compressibility of natural fracture network has little effect on the reasonable production pressure difference. By observing partial enlarged detail near the reasonable pressure difference, there is a small difference in the reasonable production pressure difference of these curves. As shown in Fig. 13, with the difference of compressibility of natural fracture network changing from 0 to 0.004 MPa^{-1} , reasonable production pressure difference is 9.8 MPa, 9.7 MPa, 9.6 MPa, 9.5 MPa, and 9.3 MPa respectively, and cumulative oil production decreases from 1598.83 to 1518.12 m^3 , which reduces by 5.05%.

Fig. 15 Reasonable production pressure difference and cumulative oil production under different angles



As a result, we can conclude that the larger the difference of compressibility of natural fracture network, the stronger the anisotropy, the smaller the reasonable production pressure difference, and the lower the cumulative oil production. Besides, the difference of compressibility of natural fracture network has less effect on the reasonable production pressure difference than that of pressure-sensitive coefficient of artificial fracture.

Direction of principal permeability

In the study, we assumed that the compressibility of two groups of natural fractures are equivalent ($C_{f1} = C_{f2} = 0.002 \text{ MPa}^{-1}$), that is, isotropic, and the direction of principal permeability does not change. The angle between artificial fractures and the direction of principal permeability are 0° , 15° , 30° , 45° , 60° , 75° , and 90° respectively by changing the direction of two groups of natural fracture networks. Then, the relationship between cumulative oil production and production pressure difference under different pressure-sensitive coefficient of artificial fracture is presented in Fig. 14. The trend of the seven curves is almost the same. By observing partial enlarged detail near the reasonable pressure difference, reasonable production pressure difference is 9.8 MPa. Therefore, we can conclude the direction of principal permeability only affects cumulative oil production and has no effect on reasonable production pressure difference.

As shown in Fig. 15, with the increase of the angle between artificial fractures and the direction of principal permeability, the cumulative oil production is also increasing. The cumulative oil production of angle 90° is 8.26% more than that of angle 0° . This is mainly because the larger the angle between the direction of principal permeability and the artificial fracture, the larger the permeability perpendicular to the direction of artificial fracture, which make fluid easier to flow into artificial fracture.

Field application

The aim of this model is to optimize production pressure difference of MFHW in tight reservoir; therefore, field application is the ultimate task. In field case analysis, a MFHW (JHW015) in a tight reservoir from Xin Jiang oilfield is studied. The basic parameters of JHW015 are shown in Table 2.

The production time is 600 days and the cumulative oil production under different production pressure difference is calculated. As shown in Fig. 16, the optimal production pressure difference is between 8 and 9 MPa. By observing partial enlarged detail, reasonable production pressure difference is 8.4 MPa and cumulative oil production is 6215.03 m^3 . Therefore, the proposal model can provide the evidences for optimal design of reasonable production pressure difference in tight reservoir.

Table 2 Basic parameters for JHW015

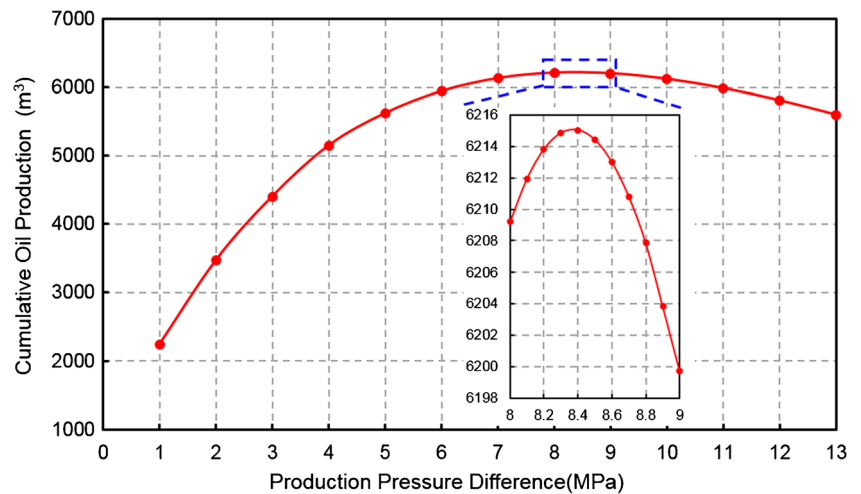
Parameters	Value
Reservoir size	1500 m × 600 m × 25 m
Permeability of artificial fractures	$70 \mu\text{m}^2$
Aperture of artificial fractures (heel and toe)	5 mm, 2 mm
Half-length of artificial fractures	130 m
Pressure-sensitive coefficient of artificial fractures	0.10 MPa^{-1}
Length of horizontal wellbore	1200 m
Number of stages	21
Direction of two sets of natural fracture (North: 0° clockwise)	$0^\circ, 150^\circ$
Compression coefficient of two sets of natural fracture	$0.002 \text{ MPa}^{-1}, 0.003 \text{ MPa}^{-1}$
Permeability of two sets of natural fracture	$67 \times 10^{-3} \mu\text{m}^2, 67 \times 10^{-3} \mu\text{m}^2$
Matrix permeability	$0.01 \times 10^{-3} \mu\text{m}^2$
Matrix porosity	0.11
Initial reservoir pressure	36.70 MPa
Oil viscosity	3.2 mPa s
Production time	600 days

Conclusions

In this study, in order to determine the main controlling factors of reasonable production pressure difference and provide guidance for optimal design of production pressure difference, a semi-analytical productivity model of MFHW considering the pressure-sensitive effect of artificial fractures and natural fractures is proposed. Some key conclusions are drawn:

1. Stress-sensitive effect cannot be ignored in the development of fractured tight reservoir. The accuracy of productivity prediction can be improved by considering the pressure-sensitive effect of artificial fractures and natural fracture networks in productivity model.
2. In the study, three factors (pressure-sensitive coefficient of artificial fracture, compressibility of natural fracture network, direction of principal permeability) for reasonable production pressure difference are analyzed. Compared with pressure-sensitive coefficient of artificial fracture, the impact of compressibility of natural fracture network and direction of principal permeability on the production pressure difference and cumulative oil production are relatively weak. Therefore, pressure-sensitive coefficient of artificial fracture is the main controlling factor.
3. Based on the research above, some suggestions can be proposed: by improving the strength of proppant to reduce the pressure-sensitivity effect of artificial fractures, cumulative production is increasing; artificial fractures should be perpendicular to the direction of principal permeability as far as possible,

Fig. 16 Cumulative oil production under different production pressure difference



which can reduce the resistance of from matrix to artificial fractures, thereby increasing productivity.

This work provides practical values for (1) predicting productivity in fractured tight reservoirs accurately and (2) analyzing main controlling factor of reasonable production pressure difference and further providing an important basis for the optimal design of reasonable production pressure difference in tight reservoir.

Funding information This work is supported by the National Basic Research 973 Program of China (2015CB250900) and Research and Application of Key Technologies for Effective Development of Volcanic Reservoirs (2017E-0405).

Nomenclature a , reservoir length, m; A , coefficient matrix; b , reservoir width, m; B , constant vector; C_{fi} , compression coefficient of i th group of natural fracture networks, MPa^{-1} ; C_t , total compressibility, MPa^{-1} ; h ,

reservoir thickness, m; i, j , sink unit number, integer; k , artificial fracture number, integer; k_m , matrix permeability, μm^2 ; k_{m0} , initial matrix permeability, μm^2 ; k_{AFi} , artificial fracture permeability, μm^2 ; k_{AF0} , initial permeability of artificial fracture, μm^2 ; k_{fi} , permeability of the i th group of natural fracture network, μm^2 ; k_{fj0} , initial permeability of the i th group of natural fracture network, μm^2 ; K , diagonal tensor permeability; K' , full tensor permeability; N , the total number of artificial fractures, integer; ns , the total number of sink unit in single wing fracture, integer; p_{klj} , the pressure drop of the j th sink unit, MPa; p_{kl0} , the pressure drop of the grid of wellbore, MPa; p_{wf} , bottom hole flow pressure, MPa; p_{ini} , initial formation pressure, MPa; ΔP , pressure difference, MPa; q , flow rate, m^3/day ; $q_{n\Delta t}$, flow rate of all sink units at the time step of $n\Delta t$, vector; r_o , equivalent grid radius, m; r_w , wellbore radius, m; t , time, month; t_0 , initial time, month; w_{fmax} , the width of fracture heel, mm; w_{fmin} , the width of fracture toe, mm; τ , time variable, month; ϕ , porosity, fraction; μ , viscosity, mPa s; α , the angle between the direction of principal permeability and the reference coordinate system, $^\circ$; α_{AFi} , pressure-sensitive coefficient of artificial fracture, MPa^{-1} ; β_i , the angle between the i th group of natural fracture network and the x -axis, $^\circ$; γ , the angle between the two coordinate systems, $^\circ$; 1, fractured left wing; 2, fractured right wing

Appendix

The detailed source functions:

$$S_1 = S_1(x_i, x_{k1,i}, \tau) = \frac{b_{fk1,i}}{a} \left[1 + \frac{4a}{\pi b_{fk1,i}} \sum_{n=1}^{+\infty} \frac{1}{n} \exp\left(-\frac{n^2 \pi^2 K_x \tau}{\alpha a^2}\right) \sin \frac{n\pi b_{fk1,i}}{2a} \cos \frac{n\pi x_{k1,i}}{a} \cos \frac{n\pi x_i}{a} \right] \tag{A-1}$$

$$S_2 = S_2(y_i, y_{k1,i}, \tau) = \frac{y_{fk1,i}}{bns} \left[1 + \frac{4bns}{\pi y_{fk1,i}} \sum_{n=1}^{+\infty} \frac{1}{n} \exp\left(-\frac{n^2 \pi^2 K_y \tau}{\alpha b^2}\right) \sin \frac{n\pi y_{fk1,i}}{2bns} \cos \frac{n\pi y_{k1,i}}{b} \cos \frac{n\pi y_i}{b} \right] \tag{A-2}$$

$$S_3 = S_3(z_i, z_{k1,i}, \tau) = 1 + \frac{4}{\pi} \sum_{n=1}^{+\infty} \frac{1}{n} \exp\left(-\frac{n^2 \pi^2 K_z \tau}{\alpha h^2}\right) \sin \frac{n\pi}{2} \cos \frac{n\pi z_{k1,i}}{h} \cos \frac{n\pi z_i}{h} \tag{A-3}$$

The coefficient matrix A :

$$A = \begin{bmatrix} A_{1,1,1}, A_{1,1,2}, \dots, A_{1,1,ns}, A_{1,2,1}, A_{1,2,2}, \dots, A_{1,2,ns}, A_{2,1,1}, A_{2,1,2}, \dots, A_{2,1,ns}, A_{2,2,1}, A_{2,2,2}, \dots, A_{2,2,ns}, \dots \dots \dots \\ A_{k,1,1}, A_{k,1,2}, \dots, A_{k,1,ns}, A_{k,2,1}, A_{k,2,2}, \dots, A_{k,2,ns}, \dots \dots \dots A_{N,1,1}, A_{N,1,2}, \dots, A_{N,1,ns}, A_{N,2,1}, A_{N,2,2}, \dots, A_{N,2,ns} \end{bmatrix}^T \tag{A-4}$$

where

$$A_{m,d,n} = [C\beta_{(1)1,1,(m)d,n}, C\beta_{(1)1,2,(m)d,n}, \dots, C\beta_{(1)1,ns,(m)d,n}, C\beta_{(1)2,1,(m)d,n}, C\beta_{(1)2,2,(m)d,n}, \dots, C\beta_{(1)2,ns,(m)d,n}, \\ C\beta_{(2)1,1,(m)d,n}, C\beta_{(2)1,2,(m)d,n}, \dots, C\beta_{(2)1,ns,(m)d,n}, C\beta_{(2)2,1,(m)d,n}, C\beta_{(2)2,2,(m)d,n}, \dots, C\beta_{(2)2,ns,(m)d,n}, \dots, \\ C\beta_{(m)1,1,(m)d,n} + D_{(m)1,1}, C\beta_{(m)1,2,(m)d,n} + \sum_{i=1}^2 D_{(m)1,i}, \dots, C\beta_{(m)1,ns,(m)d,n} + \sum_{i=1}^n D_{(m)1,i}, \dots, \\ C\beta_{(m)1,ns,(m)d,n} + \sum_{i=1}^n D_{(m)1,i}, C\beta_{(m)2,1,(m)d,n}, C\beta_{(m)2,2,(m)d,n}, \dots, C\beta_{(m)2,ns,(m)d,n}, \dots, \\ C\beta_{(N)1,1,(m)d,n}, C\beta_{(N)1,2,(m)d,n}, \dots, C\beta_{(N)1,ns,(m)d,n}, C\beta_{(N)2,1,(m)d,n}, C\beta_{(N)2,2,(m)d,n}, \dots, C\beta_{(N)2,ns,(m)d,n}] \tag{A-5}$$

$$C = \frac{1}{abh\phi C_t} \tag{A-6}$$

$$D_{(k)1,i} = \frac{\mu y_{fk1}}{k_f w_{k1,i} hns} \tag{A-7}$$

$$D_{(k)2,i} = \frac{\mu y_{fk2}}{k_f w_{k2,i} hns} \tag{A-8}$$

$$\beta_{(k)1,i,(m)d,j} = \left(\int_0^{\Delta t} (S_1 \cdot S_2 \cdot S_3)_{s1,i} d\tau \right)_{(x_{(m)d,j}, y_{(m)d,j}, z_{(m)d,j})} \tag{A-9}$$

$$\beta_{(k)2,i,(m)d,j} = \left(\int_0^{\Delta t} (S_1 \cdot S_2 \cdot S_3)_{s2,i} d\tau \right)_{(x_{(m)d,j}, y_{(m)d,j}, z_{(m)d,j})} \tag{A-10}$$

Vector B :

$$B = [\bar{p}_{(n-1)\Delta t} - P_{wf}, \bar{p}_{(n-1)\Delta t} - P_{wf}, \dots, \bar{p}_{(n-1)\Delta t} - P_{wf}]^T \tag{A-11}$$

where

$$\bar{p}_{(n-1)\Delta t} = \int_{\Gamma} p_{(n-1)\Delta t}(x, y) dS \tag{A-12}$$

$$p_{(n-1)\Delta t}(x, y) = p_{(n-2)\Delta t}(x, y) - C \sum_{s=1}^N \left(\sum_{i=1}^{ns} (q_{s1,i} \int_0^{m\Delta t} (S_1 \cdot S_2 \cdot S_3)_{s1,i} d\tau + q_{s2,i} \int_0^{m\Delta t} (S_1 \cdot S_2 \cdot S_3)_{s2,i} d\tau) \right)_{(x_{k1,j}, y_{k1,j}, z_{k1,j})} \tag{A-13}$$

References

Baba A, Tiab D (2001) Effect of finite conductivity horizontal well on transient-pressure behavior. Presented at the SPE Permian Basin Oil and Gas Recovery Conference, Midland, Texas, pp 15–17 May. SPE-70013-MS. <https://doi.org/10.2118/70013-MS>

Chen Z, Liao X (2017) A finite-conductivity horizontal-well model for pressure-transient analysis in multiple-fractured horizontal wells. SPE J 22(04):1112–1122. <https://doi.org/10.2118/177230-PA>

Cinco-Ley H, Samaniego-V F (1981) Transient pressure analysis for fractured wells. J Pet Technol 33(9):1749–1766. SPE 7490-PA. <https://doi.org/10.2118/7490-PA>

Du J, Wong R C K. (2002) Stress-induced permeability anisotropy in fractured reservoir [C]//SPE International Thermal Operations and Heavy Oil Symposium and International Horizontal Well Technology Conference. Society of Petroleum Engineers. doi: <https://doi.org/10.2118/79019-MS>

Giger FM, Reiss LH, and Jourdan AP 1984. The reservoir engineering aspects of horizontal drilling. Paper SPE 13024 presented at the SPE Annual Technical and Exhibition, Houston, 16–19 September. doi: <https://doi.org/10.2118/13024-MS>.

Gringarten AC, Ramey J, Raghavan R (1974) Unsteady-state pressure distributions created by a well with a single infinite-conductivity vertical fracture. SPE J 14(4):347–360. SPE 4051-PA. <https://doi.org/10.2118/4051-PA>

- Guo B, Schechter DS (1997) A simple and rigorous mathematical model for estimating inflow performance of wells intersecting long fractures. Paper SPE 38104 presented at the SPE Asia Pacific Oil and Gas Conference and Exhibition, Kuala Lumpur, pp 14–16. <https://doi.org/10.2118/38104-MS>
- Guo J, Heng L, Fanhui Z (2015) Influence of varying fracture width on fractured wells long-term productivity. *J China Univ Pet (Edition of Natural Science)* 39(1):111–115. <https://doi.org/10.3969/j.issn.1673-5005.2015.01.016>
- He Y, Cheng S (2017) A semianalytical methodology to diagnose the locations of underperforming hydraulic fractures through pressure-transient analysis in tight gas reservoir. *SPE J* 22(03):924–939. <https://doi.org/10.2118/185166-PA>
- He Y, Cheng S (2018) An improved rate-transient analysis model of multi-fractured horizontal wells with non-uniform hydraulic fracture properties. *Energies* 11(2):393. <https://doi.org/10.3390/en11020393>
- Karcher RJ, Giger FM, Combe J (1986) Some practical formulas to predict horizontal well behavior. Paper SPE 15430 presented at the SPE Annual Technical Conference and Exhibition, New Orleans, pp 5–8. <https://doi.org/10.2118/15430-MS>
- Li H, Jia Z, Wei Z (1996) A New method to predict performance of fractured horizontal wells. Paper SPE 37051 presented at the International Conference on Horizontal Well Technology, Calgary, pp 18–20. <https://doi.org/10.2118/37051-MS>
- Ma CY, Liu YT, Wu JL (2013) Simulated flow model of fractured anisotropic medium: permeability and fracture [J]. *Theor Appl Fract Mech* 65:28–33. <https://doi.org/10.1016/j.tafmec.2013.05.005>
- Mayerhofer MJ, Lolon EP, Warpinski NR, Cipolla CL, Walser D, Rightmire CM (2010) What is stimulated reservoir volume? *SPE Produc Oper* 25(1):89–98. SPE 119890-PA. <https://doi.org/10.2118/119890-PA>
- Ozkan E, Brown M (2013) Comparison of fractured-horizontal-well performance in tight sand and shale reservoirs. *SPE Reserv Eval Eng* 14:248–259. <https://doi.org/10.2118/121290-PA>
- Peaceman DW (1990) Interpretation of wellblock pressures in numerical reservoir simulation: part 3 – off-center and multiple wells within a wellblock. SPE16976. doi:<https://doi.org/10.2118/16976-PA>
- Penmacha VR (1997) Modeling of horizontal wells with pressure drop in the well. Stanford University
- Soliman MY, Hunt JL, El Rabaa AM (1990) Fracturing aspects of horizontal wells. *J Pet Technol* 42(8):966–973. SPE-18542-PA. <https://doi.org/10.2118/18542-PA>
- Tian L, Feng B (2019) Performance evaluation of gas production with consideration of dynamic capillary pressure in tight sandstone reservoirs. *ASME J Energy Resour Technol* 141(2):022902. <https://doi.org/10.1115/1.4041410>
- Wan J, Aziz K (2002) Semi-analytical well model of horizontal wells with multiple hydraulics fractures. *SPE J* 7(4):437–445. SPE-81190-PA. <https://doi.org/10.2118/81190-PA>
- Wei Y, Economides MJ (2005) Transverse hydraulic fractures from a horizontal well. Paper SPE 94671 presented at the SPE Annual Technical Conference and Exhibition, Dallas, pp 9–12. <https://doi.org/10.2118/94671-MS>
- Yao S, Zeng F (2013) A semi-analytical model for multi-stage fractured horizontal wells. In: SPE Unconventional Resources Conference Canada. Calgary, Alberta, Canada, pp 5–7. <https://doi.org/10.2118/167230-MS>
- Yildiz T, Ozkan E (1998) A simple correlation to predict wellbore pressure drop effects on horizontal well productivity. Presented at the SPE Annual Technical Conference and Exhibition, New Orleans, Louisiana, pp 27–30 SPE-48938-MS. <https://doi.org/10.2118/48938-MS>
- Zeng J, Wang X (2016) Analytical model for multi-fractured horizontal wells in tight sand reservoir with threshold pressure gradient. Society of Petroleum Engineers. doi:<https://doi.org/10.2118/181819-MS>
- Zhang F, Yang D (2018) Effects of non-Darcy flow and penetrating ratio on performance of horizontal wells with multiple fractures. SPE Unconventional Resources Conference Canada, 5–7 November, Calgary, Alberta, Canada. doi:<https://doi.org/10.2118/167218-MS>